Aberrant Neurogenesis After Stroke A Retroviral Cell Labeling Study

Fanny Niv, MD; Silke Keiner, PhD; Krishna-K, PhD; Otto W. Witte, MD; Dieter Chichung Lie, MD; Christoph Redecker, MD

Background and Purpose—Adult neurogenesis in the dentate gyrus is a unique form of brain plasticity that is strongly stimulated after stroke. We investigate the morphological properties of new granule cells, which are born and develop after the ischemic insult, and query whether these adult-born neurons properly integrate into the pre-existing hippocampal circuitries.

Methods—Two well-established models were used to induce either small cortical infarcts (photothrombosis model) or large territorial infarcts (transient middle cerebral artery occlusion model). New granule cells were labeled 4 days after the initial insult by intrahippocampal injection of a retroviral vector encoding green fluorescent protein and newborn neurons were morphologically analyzed using a semiautomatic Neurolucida system and confocal laser scanning microscopy at 6 weeks.

Results—Approximately 5% to 10% of newborn granule cells displayed significant morphological abnormalities comprising additional basal dendrites and, after middle cerebral artery occlusion, also ectopic cell position. The extent of morphological abnormalities was higher after large territorial infarcts and seems to depend on the severity of ischemic damage. An increased portion of mushroom spines in aberrant neurons suggests stable synaptic integration. However, poststroke generated granule cells with regular appearance also demonstrate alterations in dendritic complexity and spine morphology.

Conclusions—The remarkable stimulation of dentate neurogenesis after stroke coincides with an increased rate of aberrantly integrated neurons, which may contribute to functional impairments and, hypothetically, favor pathogenesis of adjustment disorders, cognitive deficits, or epilepsy often seen in stroke patients. (Stroke. 2012;43:2468-2475.)

Key Words: adult neurogenesis ■ dentate gyrus ■ photothrombosis ■ plasticity ■ retroviral vectors

Teurogenesis in the adult hippocampus is a unique form of structural brain plasticity modified not only by physiological stimuli, but also by brain insults such as stroke, epilepsy, and traumatic brain injury. Within the dentate gyrus, the generation, migration, differentiation, and maturation of newborn neurons appear to be precisely regulated thereby allowing proper integration of the neurons into the preexisting hippocampal network.1-3 After brain ischemia, proliferation and differentiation of neuronal progenitors in the subgranular zone of the dentate gyrus (DG) is strongly stimulated, leading to a significant increase in neurogenesis.4-6 To date, it is unclear whether the abundance of newborn neurons generated after stroke properly integrates into the hippocampal network. Experimental status epilepticus is also a powerful stimulator of adult neurogenesis in the DG^{7,8}; however, it disrupts integration of these new granule

cells within the hippocampal network.⁹⁻¹¹ Jessberger et al¹⁰ described a significant number of newborn neurons showing an aberrant morphology comprising additional basal dendrites directed into the hilus and, in some cases, an ectopic positioning of the newborn cells. These morphological changes are known to give rise to increased recurrent excitatory circuitry^{12,13} and may represent a pivotal component of the epileptic disease process.

In this study, we investigated the fine morphology of newborn neurons generated after stroke as an indicator of structural integration into the pre-existing network. For this purpose, we used retroviral cell labeling, which allows a detailed morphological reconstruction of dendrites and spines of newborn neurons to investigate poststroke neurogenesis in small circumscribed cortical infarcts and large ischemic infarcts in the middle cerebral artery territory. Our results indicate that stroke

Received April 14, 2012; accepted May 18, 2012.

© 2012 American Heart Association, Inc.

From the Hans Berger Department of Neurology, Jena University Hospital, Jena, Germany (F.N., S.K., K.K., O.W.W., C.R.); Research Group Adult Neurogenesis and Neural Stem Cells, Institute of Developmental Genetics, Helmholtz Zentrum München, German Research Center for Environmental Health, Neuherberg, Germany (C.D.L.); and the Institute of Biochemistry, Emil Fischer Center, University Erlangen-Nürnberg, Erlangen, Germany (C.D.L.)

The online-only Data Supplement is available with this article at http://stroke.ahajournals.org/lookup/suppl/doi:10.1161/STROKEAHA.112.660977/-/DC1.

Correspondence to Christoph Redecker, MD, Hans Berger Department of Neurology, Jena University Hospital, Erlanger Allee 101, 07747 Jena, Germany. E-mail redecker@med.uni-jena.de

leads to a morphologically aberrant integration of adult newborn cells in the DG, in which the extent of abnormalities increased with the size of ischemic damage.

Materials and Methods

Infarct Induction

The study was performed on a total number of 43 male Wistar rats. Animals were held under standard housing conditions in ordinary cages (4 animals/cage). Food and water were provided ad libitum. All experimental procedures were approved by the German Animal Care and Use Committee in accordance with the European Directives.

Photothrombosis Model

After anesthesia using 2.5% to 3.5% isoflurane in a mixture of $\rm O_2/N_2O$, animals were placed in a stereotactic frame, the scalp was incised, and an optic fiber bundle (2.4 mm diameter) connected to a cold light source (Schott KL 1500, Mainz, Germany) was positioned on the skull 0.5 mm anterior to bregma and 3.7 mm lateral to the midline above the forelimb sensorimotor cortex. Immediately after onset of illumination (duration, 20 minutes), Rose Bengal (1.3 mg/100 mg body weight in 0.9% NaCl) was injected through a femoral vein catheter. Throughout surgery, body temperature was kept constant at 36.5°C. Sham-operated animals received the same treatment without illumination of the brain.

Middle Cerebral Artery Occlusion Model

After anesthesia, as described previously, the common carotid, external carotid, and pterygopalatine arteries were exposed and ligated on the right side. The right internal carotid artery was occluded with a microsurgical clip and subsequently an arteriotomy was performed in the common carotid artery. A 3.0-monofilament suture (Doccol) with a rounded tip was inserted into the common carotid artery and advanced through the internal carotid artery to the ostium to occlude the middle cerebral artery. After 60 minutes, the suture was removed, the wound was closed, and the rats were allowed to recover. Sham-operated animals (=control) received the same treatment without occlusion of the right internal carotid artery.

Retroviral Vectors

We used the retroviral vectors CAG-green fluorescent protein (GFP) and CAG-red fluorescent protein (RFP) to label newly generated granule neurons in the right DG.¹⁴ Viral vectors were produced by cotransfecting HEK 293 T cells with pCAG-GFP/pCAG-RFP and the packing constructs pCMV VSVg and pCMVpg¹⁵ at a final titer of approximately 1×10^7 colony-forming units/mL.

Experimental Design

In a first set of experiments, we investigated the morphology of newborn granule cells generated after experimental ischemic infarcts: rats (n=28, weight 250-270 g) were randomly divided into 4 experimental groups and either underwent photothrombosis (PT; n=6), PT sham surgery (n=6, PT control), middle cerebral artery occlusion (MCAO; n=10), or MCAO sham surgery (n=6, MCAO control) in the right hemisphere on day P90. Four days later (P94), the animals received a stereotaxic injection of the CAG-GFP retrovirus into the dentate gyrus (1 μ L virus, x=3.1 mm; y=1.5 mm; z=4.0 mm according to bregma) and were allowed to recover for 6 weeks. In a second series of experiments, we further analyzed whether resident neurons born weeks before the infarct show similar morphological properties compared with adult newborn neurons generated after stroke. For this purpose, P14 rats (n=15, weight 20-25 g) received a first stereotaxic injection of CAG-RFP retroviral vector in the right dentate gyrus (1 μ L virus, x=2.7 mm; y=1.0 mm; z=3.4 mm according to bregma). Four days after either PT (n=7) or MCAO (n=8) procedures, on P94, a second CAG-GFP retroviral vector injection was given as described previously. On day P132, all rats were anesthetized with diethylether and perfused transcardially

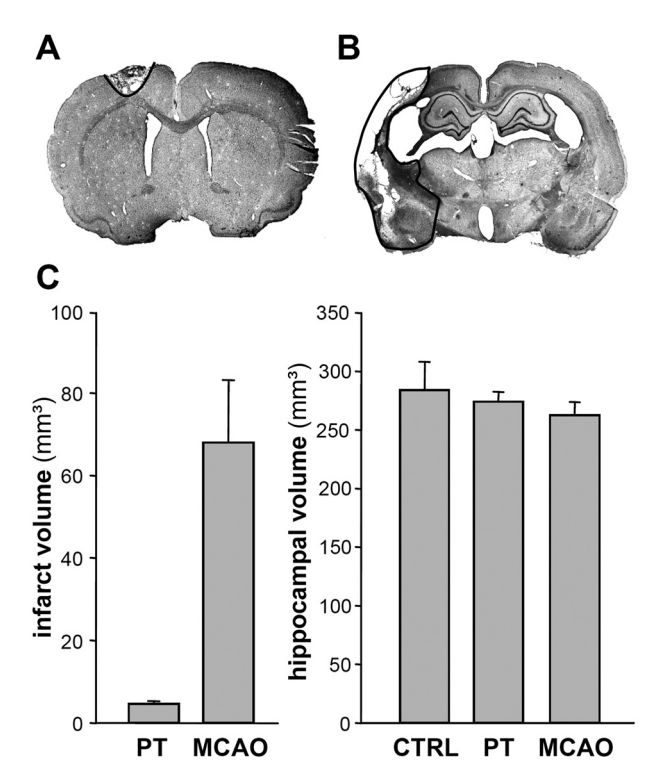


Figure 1. Morphology of experimental stroke. **A**, Photothrombotic cortical infarcts (PT). **B**, Stroke induced by transient middle cerebral artery occlusion (MCAO). **C**, Infarct and hippocampal volumetry 6 weeks after infarct induction. Bars represent mean±SEM.

with 4% phosphate-buffered paraformaldehyde. No animals were excluded from further analysis.

Immunohistochemistry

After transcardial perfusion, brains were postfixed in paraformaldehyde and 40-µm thick sections were sliced. Immunocytochemistry was performed using a standard peroxidase technique and doublelabeling immunofluorescence methods as described previously.16 The following primary antibodies were used: goat anti-GFP antibody (1:500; Acris, Herford, Germany), chicken anti-GFP antibody (1:1000; Aves Labs), rabbit anti-RFP antibody (1:500; Abcam, Cambridge, UK), mouse antineuronal nuclei antigen (1:500; Chemicon, Temecula, CA), and goat antisynapsin I antibody (1:500; Santa Cruz, Santa Cruz, CA). Secondary antibodies: Cy5 antimouse and CY3 antirabbit (1:250; Dianova, Hamburg, Germany), Alexa Fluor 488 antigoat, and Alexa Fluor 488 antimouse (1:250; Molecular Probes, Leiden, The Netherlands) and fluorescein isothiocyanate antichicken (1:250; Chemicon). Standard peroxidase stained cells were evaluated by light microscopy, whereas double-labeled cells were analyzed by confocal laser scanning microscopy.

Quantification and Morphological Analyses

Volumetry

Infarct and hippocampal volumes were measured in every eighth cresyl violet-stained section (40 μ m). Volumes were calculated by multiplying the appropriate region with the section interval thickness.

Quantification

Peroxidase-stained GFP-positive cells were counted in every sixth section of the complete ipsilateral DG. Phenotypes of GFP-positive cells were determined by light microscopy and percentages of cells with morphological abnormalities (aberrant newborn neurons) were quantified. Two different types of aberrant morphologies of newborn neurons were defined: (1) bipolar cells in the granule layer of the DG

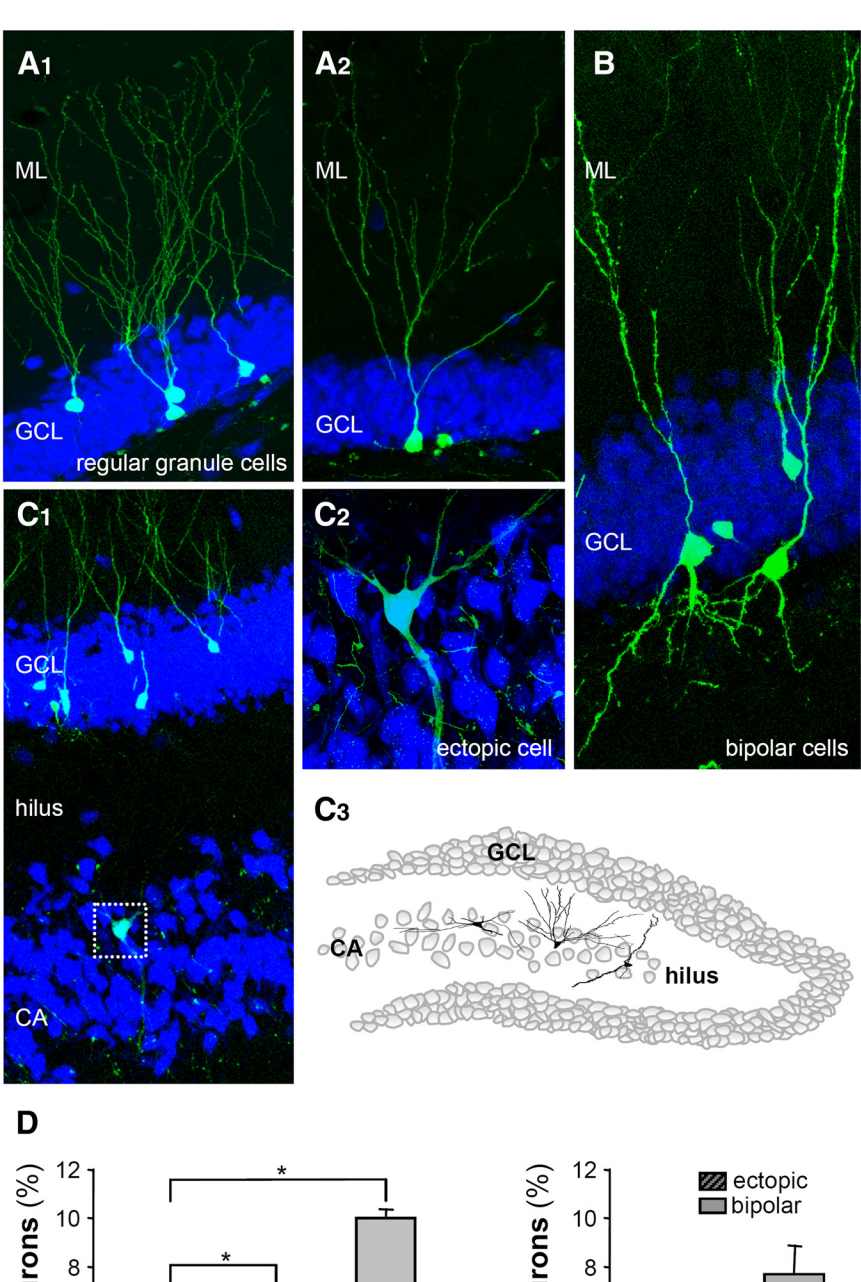
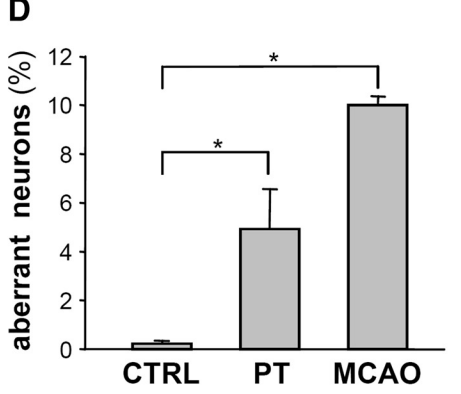
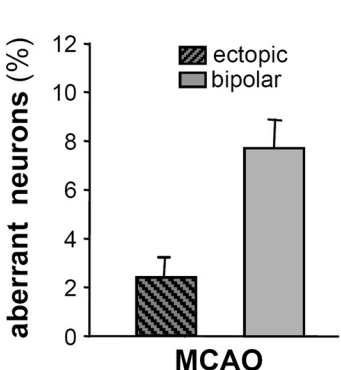


Figure 2. Retrovirally labeled newborn neurons generated after stroke. A, Examples of newborn GFP-positive neurons with regular gross morphology (A1-A2). Double-labeling of GFP (green) and NeuN (blue). B-C, Examples of newborn neurons with aberrant morphology comprising additional basal dendrites toward the hilus (bipolar cells, B) or ectopic position within the extension of cornu ammonis (CA, C1). C2, Magnification of an ectopic neuron. C3, Schematic illustration of the distribution of ectopic neurons. D, Percentage of neurons with aberrant morphology in the different experimental groups (right diagram) and percentage of ectopic and bipolar neurons in the MCAO group (left diagram). Bars represent mean ± SEM. Asterisks indicate significant differences (P<0.05). GFP indicates green fluorescent protein; GCL, granule cell layer; MCAO, middle cerebral artery occlusion; ML, molecular layer; NeuN, neuronal nuclei; PT, photothrombotic infarcts.





with basal dendritic processes directed toward the hilus; and (2) ectopically positioned cells located either beneath the subgranular zone in the hilus or in the extension of the adjacent CA region.

Dendrite Analysis

For analysis of dendritic complexity of newborn neurons, a subset of randomly selected GFP-positive cells (10-17 cells per group) from the different experimental groups (control, PT, MCAO) were morphologically reconstructed using a semiautomatic Neurolucida system (MicroBrightfield, Colchester, VT) under a 63× oil lens magnification. In addition, we analyzed a subset of RFP-positive neurons

retrovirally labeled at P14 to compare resident granule cells with newborn neurons (17 cells). Parameters evaluated included branch order, number of apical dendrites, and apical dendritic length. Axonal processes could be easily distinguished from dendrites because of their smaller diameter and lack of dendritic spines.

Spine Analysis

Spinal analysis was performed using confocal laser scanning microscopy (LSM 710; Carl Zeiss, Jena, Germany) as described previously.^{9,17} Here, a dendritic segment (second branch order) measuring $50~\mu m$ was analyzed and the total number of spines per $50~\mu m$ was quantified. According to their tip diameter, further differentiation into thin (0.25–0.6 μ m) and mushroom spines (>0.6 μ m) was undertaken.

Statistical Analysis

Statistical analysis of cell counts was performed using one-way analysis of variance followed by the Tukey-Kramer post hoc analysis for multiple comparisons. Data are presented as mean±SEM.

Results

Morphology of Newborn Neurons Generated After Stroke

All animals with photothrombotic stroke had typical cortical infarcts located in the forelimb sensorimotor cortex according to Paxinos and Watson.¹⁸ Correspondingly, animals that underwent transient MCAO showed infarcts covering the right middle cerebral artery territory including cortex and basal ganglia, except the hippocampus formation (Figure 1A). Infarct volumetry revealed significantly smaller infarcts after PT (4.85±0.59 mm³) compared with MCAO (68.17±15.16 mm³; Figure 1B). Additional volumetry of the hippocampal formation revealed no differences between the experimental groups (Figure 1C).

Six weeks after CAG-GFP injection, the majority of newborn neurons generated after stroke demonstrated typical gross morphological properties of granule cells (approximately 90%–95%) analogous to control animals. Namely, the dendrites of these newborn neurons showed a highly polarized morphology and apical dendritic processes with abundant spines extending into the molecular layer. Furthermore, axons reached their target area, CA3, through the mossy fiber pathway, indicating a regular integration into the hippocampal circuitry.^{2,19} However, a small fraction of newborn neurons (5%-10%) displayed notable differences in neuronal morphology. In addition to the apical dendrites, a basal dendrite or even dendritic arborization was observed, which resulted in bipolar morphology. These morphological aberrations were detected after both PT (4.97% $\pm 1.62\%$; P=0.04) as well as MCAO (10.05% \pm 0.34%; P=0,007) and were mostly absent in control animals $(0.27\pm0.1\%)$, where only one single bipolar neuron was identified (Figure 2; onlineonly Data Supplement Table I) as found in the physiological state and described in the literature.²⁰ The number of aberrant newborn neurons appeared to be higher in animals with large territorial infarcts (MCAO) compared with those with small cortical infarcts (PT), but this difference did not reach significance. Furthermore, we detected newborn neurons ectopically located in the extension of the cornu ammonis adjacent to the hilus (Figure 2C). These ectopic neurons were exclusively found in MCAO animals, possibly indicating an aberrant migration or even ectopic neurogenesis (Figure 2C-D).

Dendritic Morphology

Although the majority of newborn cells after cerebral ischemia appear to form regular morphological characteristics, detailed analyses of dendritic complexity revealed several disparities in newborn neurons generated after MCAO (Figure 3; online-only Data Supplement Table I). Specifically,

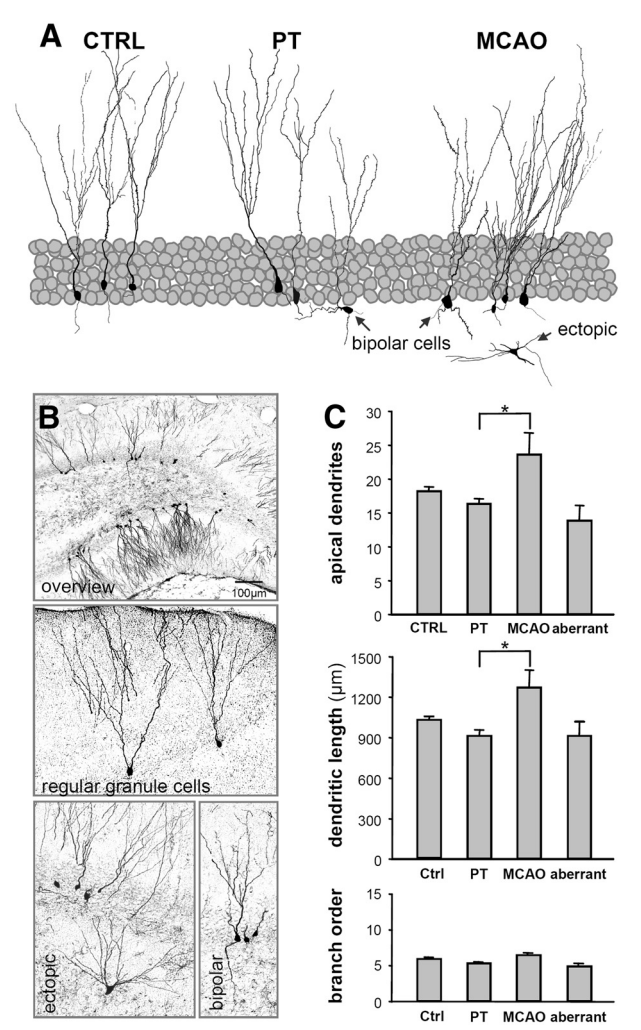


Figure 3. Dendritic morphology of newborn neurons generated in the DG after stroke. **A**, Neurolucida reconstruction of GFP-positive neurons in the different experimental groups. Neurons with bipolar morphology were observed after PT and MCAO, whereas ectopic neurons were exclusively found after MCAO. **B**, Peroxidase-stained sections demonstrating GFP-positive newborn neurons with regular and aberrant morphology in situ. **C**, Quantification of apical dendrites, dendritic length, and branch order in the different groups of neurons showing a significant difference in dendritic complexity between PT and MCAO. Bars represent mean±SEM. Asterisks indicate significant differences (P<0.05). DG indicates dentate gyrus; GFP, green fluorescent protein; PT, photothrombosis; MCAO, middle cerebral artery occlusion.

newborn neurons with regular polarity and location within the DG displayed an increase in number of apical dendrites and the dendritic length (Figure 3). These morphological differences were only observed in animals that had undergone MCAO. Newborn granule cells in PT animals and even aberrant neurons from PT or MCAO animals did not show any differences in number of apical dendrites and dendritic length compared with sham-operated controls (Figure 3). Further analysis of the highest branch order did not reveal any significant difference between the groups. Taking together, new neurons born after MCAO showed a significant increased complexity.

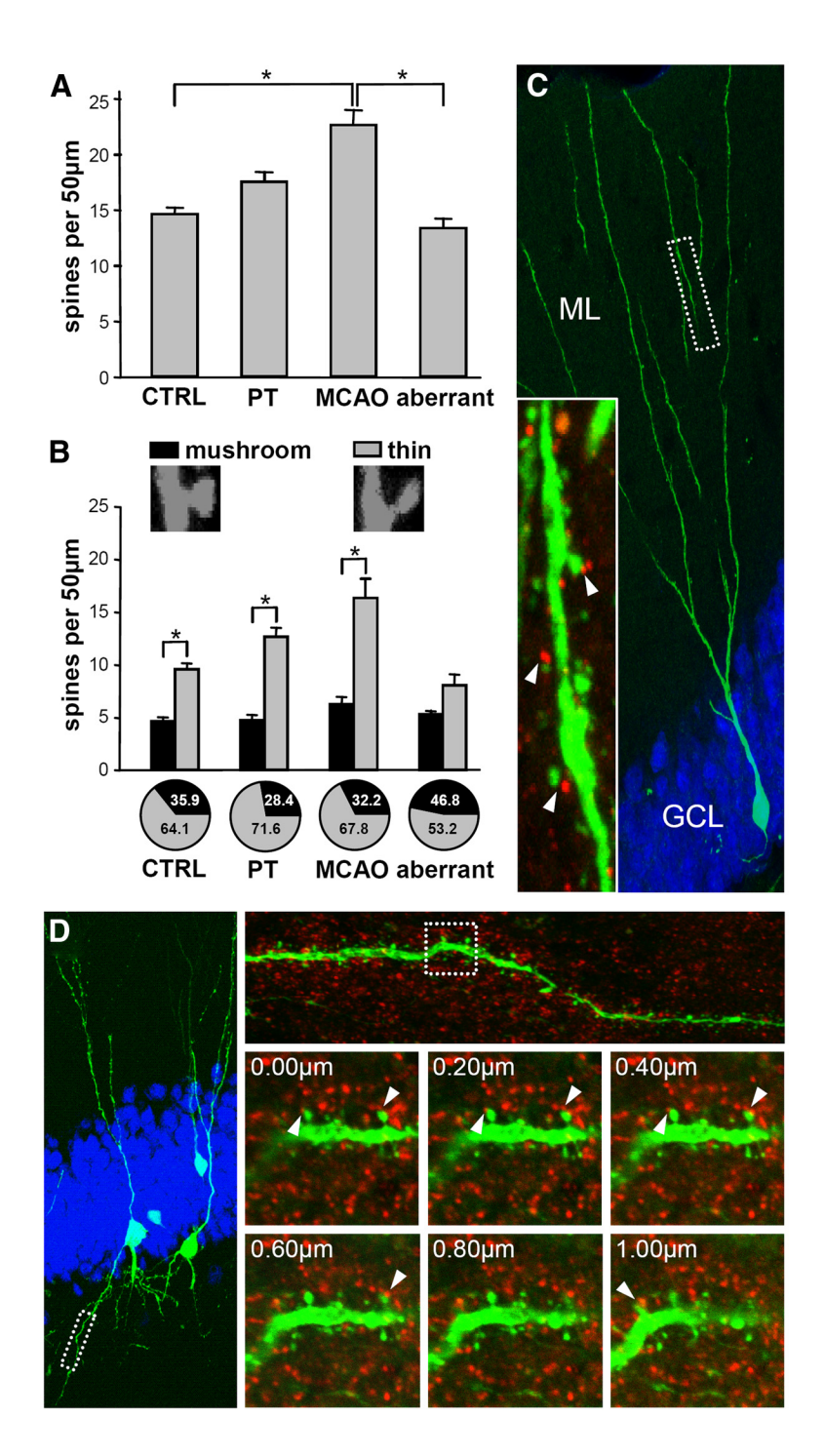


Figure 4. Spine density and synaptic integration of newborn neurons generated in the DG after stroke. A, Quantification of spine numbers in regularly formed neurons from CTRL, PT, and MCAO animals and aberrant neurons from PT and MCAO animals (see online-only Data Supplement Table I). B, Numbers of dendritic thin and mushroom spines in the different groups of neurons. High-resolution confocal images of a mushroom spine (tip diameter $> 0.6 \mu m$) and a thin spine. Pie charts display the ratio between thin and mushroom spines. Bars represent mean ± SEM. Asterisks indicate significant differences (P<0.05). C, Confocal images of dendrites of regular newborn granule neurons generated after MCAO. Inset, Spiny processes on dendrites extending from this neuron were often in close proximity (arrowheads) to the presynaptic protein synapsin (red). D, Basal dendritic spines from aberrant neurons were also commonly juxtaposed to synapsin punctate (arrowheads, Z-stack). DG indicates dentate gyrus; CTRL, control; PT, photothrombosis; MCAO, middle cerebral artery occlusion.

Spine Morphology

A detailed characterization of spine morphology additionally demonstrated that the density of spines was significantly increased in newborn neurons generated after MCAO (Figure 4A–B). This difference was absent in newborn granule cells from PT animals and also in aberrantly integrated neurons from PT or MCAO animals (Figure 4A). Further analysis of spine morphology showed a significant majority of thin spines (64.1%–71.5%) compared with mushroom spines (28.4%–35.9%) on newly generated neurons from PT, MCAO as well as control animals (Figure 4B). In contrast, aberrant neurons showed a balanced ratio of thin (53.2%)

and mushroom spines (46.8%). Taking into account that mushroom spines reflect established synaptic contacts, our findings suggest that not only new neurons with regular gross morphology, but also aberrant neurons were stably integrated. Additional immunocytochemical staining with antibodies against the presynaptic marker protein synapsin confirmed this observation (Figure 4C–D). Dendritic spines in the molecular layer of control granule cells were commonly juxtaposed to synapsin punctate (Figure 4C). The same was true for spines on basal dendrites arising from aberrant bipolar neurons born after stroke (Figure 4D).

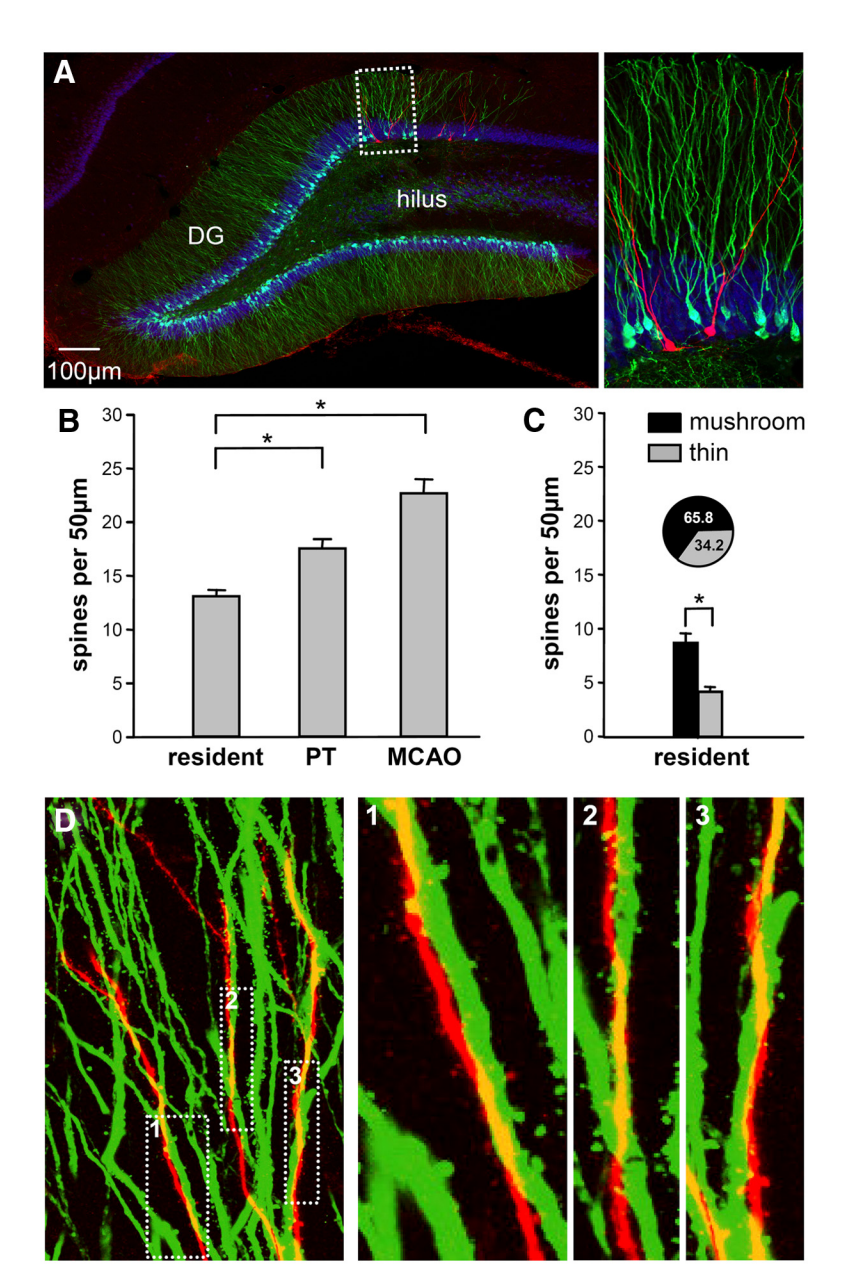


Figure 5. Comparison of newborn neurons generated after MCAO with resident neurons born at postnatal Day 14 (P14). **A**, Confocal image of DG showing resident neurons (green) generated at P14 and newborn neurons born 4 days after MCAO at P94 (red, dotted frame). **B**, Quantification of spine numbers. **C**, Numbers of dendritic thin and mushroom spines on resident neurons. Pie charts display the ratio between thin and mushroom spines. Bars represent mean \pm SEM. Asterisks indicate significant differences (P<0.05). **D**, Comparison of dendrite morphology in the ML between resident (green) and poststroke generated (red) neurons. MCAO indicates middle cerebral artery occlusion; DG, dentate gyrus; ML, molecular layer.

Comparison With Resident Granule Cells Generated Before Stroke

In an additional set of experiments, we addressed the question whether newborn neurons generated after stroke display morphological disparities compared with resident granule cells born weeks before the ischemic insult at P14 (Figure 5A). The early injection of the CAG-RFP retroviral vector at P14 labeled a huge population of granule cells, making the mossy fiber path and axonal endings in the CA3 region effortless visible. Aberrant RFP-positive neurons were not detected. A detailed morphological comparison of these resident granule cells with new poststroke and adult control neurons revealed no differences in branch order, number of apical dendrites, and dendritic length (online-only Data Supplement Table I). However, resident neurons exhibited significantly less dendritic spines compared with newly generated neurons in PT or MCAO animals (Figure 5B) but displayed no difference in spine density compared with adult-born control neurons. The highest percentage of mushroom spines and generally thicker dendrites (Figure 5C–D) further indicates that these early-born neurons possess wellestablished synaptic connections within the hippocampal circuitry.

Discussion

The present study clearly demonstrates that focal brain ischemia impairs correct morphological integration of newly generated neurons in the DG. A certain fraction of newborn neurons displayed aberrant features involving bipolar dendritic arborizations and ectopic location. Bipolar neurons were detected after photothrombotic cortical infarcts as well as after large territorial stroke in the middle cerebral artery territory, whereas a small number of ectopic new neurons were exclusively found after MCAO. Detailed spine analysis further demonstrated a significant portion of mushroom spines in aberrant neurons as an indicator of stable synaptic

integration. However, poststroke-generated granule cells with regular appearance also demonstrate considerable alterations in dendritic complexity and spine morphology after MCAO.

In the physiological state, newborn neurons in the adult DG undergo a complex series of events before fully integrating in the pre-existing network and, thus, becoming seemingly indistinguishable from neurons born during embryogenesis.²⁰ Several days after cell division, newborn neurons start extending axonal and dendritic processes and receiving their first GABAergic inputs.21 Thereafter, newborn neurons obtain their first glutamatergic input and form their first glutamatergic output on CA3 pyramidal cells. This period is followed by maximal dendritic spine growth and motility as well as enhanced synaptic plasticity until the new granule cells develop relatively stable synaptic contacts between the fourth and sixth week after birth. This delicately regulated integration of new neurons into the pre-existing hippocampal network functions well in the intact brain demonstrating <1% of new neurons with aberrant connections.²²

Using 2 different models of experimental stroke, we show that a fraction of newborn neurons generated after the ischemic insult develops aberrant dendritic connections. A few of these abnormal neurons form dendrites toward the hilus, and others become positioned ectopically. Although the latter process only occurs after large cortical and subcortical infarcts (MCAO), bipolar neurons were observed after small cortical infarcts (PT) as well as after MCAO. Regular as well as aberrant neurons display a high ratio of mushroom spines closely positioned to synapsin-positive punctate. Even in the absence of electrophysiological data, these morphological findings suggest functional integration. Comparison of the quantitative and qualitative alterations in neuronal morphology between the stroke models further implies that the extent of aberrant neurogenesis depends on the size of ischemic damage. Photochemically induced cortical infarcts induce an average increase in dentate neurogenesis of approximately 50% in different experimental settings, whereas large cortical/subcortical infarcts in the middle cerebral artery territory duplicate or even triplicate the number of newborn neurons. It can be hypothesized that the DG is not capable of integrating this abundance of newborn neurons leading to aberrant dendritic sprouting and incorrect connections. Our data possibly underline this premise, but further evidence for this hypothesis can be derived from hippocampal epilepsy models. After status epilepticus, dentate neurogenesis is massively boosted leading to a roughly 20% increase of bipolar and ectopic granule cells and to additional changes in mossy fiber sprouting.8-10

Notably, newborn neurons with regular gross morphology also display significant changes in dendritic complexity (raised number and length of apical dendrites) after MCAO and—compared with resident neurons—increased spine density in both models. These morphological alterations might reflect functional changes on afferent synapses and, at least in part, also display different developmental stages. How newly generated granule cells in the DG develop after focal stroke and functionally modulate the existing hippocampal circuitries depends not only on morphological connections, but also on the functional properties of the new neurons. Evidence from different epilepsy models suggests that new neurons born in a pathological environment exhibit a high degree of plasticity at their afferent synapses.²³ Granule cells born after electrically induced status epilepticus show more inhibitory and less excitatory drive,23 whereas granule cells generated after an epileptic insult and exposed to repeated seizures during their differentiation exhibit increased synaptic excitability.²⁴ The present electrophysiological data in epilepsy models suggest that adult-born neurons have mechanisms to counteract or adapt to pathologies at their afferent synaptic inputs. To shed more light on the putative complex functional properties of adult-born postischemic granule cells, further electrophysiological investigations are needed.

Our findings of aberrant neurogenesis and subtle morphological differences of regular granule cells in 2 models of ischemic stroke support the assumption that massive increases in neurogenesis do not necessarily result in better hippocampal performance. This is in line with very heterogeneous behavioral assessments of hippocampal function in different stroke and stroke-related models in which strong enhancement of neurogenesis has been reported. Aberrant neurogenesis may contribute to functional impairments and, hypothetically, play a role in the pathogenesis of adjustment disorders, cognitive deficits, or epilepsy often seen in clinical patients with stroke. Experimental data only demonstrated better functional outcomes in animals with increased levels of neurogenesis after photothrombotic stroke²⁵ or MCAO²⁶ when different types of rehabilitative training were applied. Whether these therapeutic interventions prevent or diminish aberrant neurogenesis should be a matter of further investigations.

Acknowledgments

We thank Katrin Wassmer, Svetlana Tausch, Diana Freitag, Claudia Sommer, and Julia Oberland for excellent technical assistance. We thank Nasim Kroegel for editing the manuscript.

Sources of Funding

This work was supported by Interdisciplinary Center for Clinical Research (IZKF) Jena and German Ministry of Education and Research (BMBF program "Cell-based, regenerative therapies," 01GN0977).

Disclosures

None.

References

- 1. Zhao C, Deng W, Gage FH. Mechanisms and functional implications of adult neurogenesis. Cell. 2008;132:645-660.
- 2. van Praag H, Schinder AF, Christie BR, Toni N, Palmer TD, Gage FH. Functional neurogenesis in the adult hippocampus. Nature. 2002;415: 1030-1034.
- 3. Laplagne DA, Espósito MS, Piatti VC, Morgenstern NA, Zhao C, van Praag H, et al. Functional convergence of neurons generated in the developing and adult hippocampus. PloS Biol. 2006;4:2349-2360.
- 4. Liu J, Solway K, Messing RO, Sharp FR. Increased neurogenesis in the dentate gyrus after transient global ischemia in gerbils. J Neurosci. 1998;18:7768-7778.
- 5. Kernie SG, Parent JM. Forebrain neurogenesis after focal ischemic and traumatic brain injury. Neurol Biol Dis. 2010;37:267-274.
- 6. Arvidsson A, Kokaia Z, Lindvall O. N-methyl-D-aspartate receptormediated increase of neurogenesis in adult rat dentate gyrus following stroke. Eur J Neurosci. 2001;14:10-18.
- 7. Parent JM, Yu TW, Leibowitz RT, Geschwind DH, Sloviter RS, Lowenstein DH. Dentate granule cell neurogenesis is increased by seizures

- and contributes to aberrant network reorganization in the adult rat hip-pocampus. *J Neurosci*. 1997;17:3727–3738.
- Jessberger S, Nakashima K, Clemenson GD Jr, Mejia E, Mathews E, Ure K, et al. Epigenetic modulation of seizure-induced neurogenesis and cognitive decline. *J Neurosci*. 2007;27:5967–5975.
- Walter C, Murphy BL, Pun RY, Spieles-Engemann AL, Danzer SC. Pilocarpine-induced seizures cause selective time-dependent changes to adult-generated hippocampal dentate granule cells. *J Neurosci*. 2007;27: 7541–7552
- Jessberger S, Zhao C, Toni N, Clemenson GD Jr, Li Y Gage FH. Seizure-associated, aberrant neurogenesis in adult rats characterized with retrovirus-mediated cell labeling. *J Neurosci*. 2007;27:9400–9407.
- Kron MM, Zhang H, Parent JM. The developmental stage of dentate granule cells dictates their contribution to seizure-induced plasticity. *J Neurosci.* 2010;30:2051–2059.
- Ribak CE, Tran PH, Spigelman I, Okazaki MM, Nadler JV. Status epilepticus-induced hilar basal dendrites on rodent granule cells contribute to recurrent excitatory circuitry. *J Comp Neurol*. 2000;428: 240–253.
- Thind KK, Ribak CE, Buckmaster PS. Synaptic input to dentate granule cell basal dendrites in a rat model of temporal lobe epilepsy. *J Comp Neurol*. 2008;509:190–202.
- Jagasia R, Steib K, Englberger E, Herold S, Faus-Kessler T, Saxe M, et al. GABA-cAMP response element-binding protein signaling regulates maturation and survival of newly generated neurons in the adult hippocampus. *J Neurosci*. 2009;29:7966–7977.
- Tashiro A, Zhao C, Gage FH. Retrovirus-mediated single-cell gene knockout technique in adult newborn neurons in vivo. *Nat Protocols*. 2006:1:3049–3055.
- Kluska MM, Witte OW, Bolz J, Redecker C. Neurogenesis in the adult dentate gyrus after cortical infarcts: effects of infarct location, NMDA

- receptor blockade and anti-inflammatory treatment. *Neuroscience*. 2005; 135:723–735.
- Toni N, Teng EM, Bushong EA, Aimone JB, Zhao C, Consiglio A, et al. Synapse formation on neurons born in the adult hippocampus. *Nat Neurosci*. 2007:10:727–734.
- Paxinos G, Watson C. The Rats in the Stereotaxic Coordinates. New York, NY: Academic Press; 1986.
- Zhao C, Teng EM, Summers RG Jr, Ming GL, Gage FH. Distinct morphological stages of dentate granule neuron maturation in the adult mouse hippocampus. *J Neurosci*. 2006;26:3–11.
- Toni N, Sultan S. Synapse formation on adult-born hippocampal neurons. Eur J Neurosci. 2011;33:1062–1068.
- Ge S, Goh EL, Sailor KA, Kitabatake Y, Ming GL, Song H. GABA regulates synaptic integration of newly generated neurons in the adult brain. *Nature*. 2006;439:589–593.
- Shapiro LA, Ribak CE, Jessberger S. Structural changes for adult-born dentate granule cells after status epilepticus. *Epilepsia*. 2008;49(suppl 5): 13–18
- Jakubs K, Nanobashvili A, Bonde S, Ekdahl CT, Kokaia Z, Kokaia M, et al. Environment matters: synaptic properties of neurons born in the epileptic adult brain develop to reduce excitability. *Neuron*. 2006;52: 1047–1059.
- Wood JC, Jackson JS, Jakubs K, Chapman KZ, Ekdahl CT, et al. Functional integration of new hippocampal neurons following insults to the adult brain is determined by characteristics of pathological environment. *Exp Neurol.* 2011;229:484–493.
- Wurm F, Keiner S, Kunze A, Witte OW, Redecker C. Effects of skilled forelimb training on hippocampal neurogenesis and spatial learning after focal cortical infarcts in the adult rat brain. Stroke. 2007;38:2833–2840.
- Zhao C, Wang J, Zhao S, Nie Y. Constraint-induced movement therapy enhanced neurogenesis and behavioral recovery after stroke in adult rats. *Tohoku J Exp Med*. 2009;218:301–308.